TECHNICAL NOTE
D-312

EFFECTS OF FIXING BOUNDARY-LAYER TRANSITION FOR A SWEPT- AND A TRIANGULAR-WING AND BODY COMBINATION AT MACH NUMBERS FROM 0.60 TO 1.40

By Louis S. Stivers, Jr.

Ames Research Center
Moffett Field, Calif.

NATIONAL AERONAUTICS AND SPACE ADMINISTRATION

WASHINGTON June 1960

NATIONAL AERONAUTICS AND SPACE ADMINISTRATION

TECHNICAL NOTE D-312

EFFECTS OF FIXING BOUNDARY-LAYER TRANSITION FOR A SWEPT- AND A TRIANGULAR-WING AND BODY COMBINATION AT MACH NUMBERS FROM 0.60 TO 1.40

By Louis S. Stivers, Jr.

SUMMARY

The aerodynamic effects of fixing boundary-layer transition for a swept- and a triangular-wing configuration have been determined from tests of two small-scale wing-body models. The wings had an aspect ratio of 2.99 and 3-percent-thick biconvex sections. Lift, pitching-moment, and drag data were obtained at Mach numbers ranging from 0.60 to 1.40 for angles of attack between -2° and about 15°. The Reynolds number of the tests was generally 1.5 million; however, minimum drag measurements were made for both models over a range of Reynolds numbers from 1.0 million to about 3.0 or 4.0 million.

The effects of fixing transition for the swept- and triangular-wing configurations were generally insignificant, although for both configurations small reductions in the variations of pitching-moment curve slope with Mach number were observed at zero lift for the higher subsonic Mach numbers. Since very pronounced effects of fixing transition have been observed for an unswept-wing configuration (reported in NACA TN 4228), it is apparent that significant effects of fixing transition at transonic Mach numbers are to be expected only for wings having little or no sweep.

The relatively large increments of minimum drag coefficient due to fixing transition for both configurations at Reynolds numbers of about 1.0 million were substantially reduced as the Reynolds number was increased to about 3.0 or 4.0 million. A comparison of calculated and measured effects of Reynolds number indicated that the measured minimum drag coefficients could be extrapolated to full-scale Reynolds numbers much more reliably when transition was fixed on the models than when left free.

INTRODUCTION

In the investigation reported in reference 1 it was found that the pitching-moment and lift-curve slopes of a small-scale, unswept-wing configuration differed significantly at transonic Mach numbers, depending on whether the boundary-layer transition was left free or was fixed in a

forward location. Since the location of free transition on the full-scale aircraft is not likely to be relatively as far rearward as that on the scale model at low Reynolds numbers, it is apparent, then, that for tests of unswept-wing models at transonic Mach numbers, transition should be fixed at a location corresponding to that expected in flight.

In view of these results, a similar investigation has been conducted for both a swept- and a triangular-wing configuration. The models for both configurations had wings with the same airfoil section (3 percent thick biconvex) and essentially the same aspect ratio (2.99) as the wing of the unswept-wing model. The swept wing also had practically the same taper ratio (0.40) as did the unswept wing. This report presents the results of the investigation of the swept- and triangular-wing configurations.

NOTATION

C_D	drag coefficient
$C_{D_{min}}$	minimum drag coefficient, C_D at $\alpha = 0^\circ$
C_L	lift coefficient
C_{L_α}	lift curve slope, $\frac{\partial C_L}{\partial \alpha}$
C_m	pitching-moment coefficient referred to $\frac{\bar{c}}{4}$ (see fig. 1)
$C_{m_{C_L}}$	pitching-moment curve slope, $\frac{\partial C_m}{\partial C_L}$
$\bar{c}$	mean aerodynamic chord of wing
M	free-stream Mach number
R	Reynolds number
α	angle of attack, deg

APPARATUS AND TESTS

Models

The configurations of the swept- and triangular-wing models used in the present tests are shown in figure 1 together with pertinent geometric information. Each model was constructed of steel. The wing panels had biconvex sections and were fixed on the body at zero incidence with no dihedral.

Transition was fixed on the models by means of a 0.004-inch-diameter wire attached to the model surfaces by means of clear lacquer. On the body a transition wire ring was located at a station 1.33 inches from the apex of the body nose. On both wings the transition wires were located on the upper and lower surfaces along the 15-percent chord lines.

Wind Tunnel and Model Support

The present investigation was conducted in the Ames 2- by 2-Foot Transonic Wind Tunnel, which has a flexible nozzle and porous test-section walls that permit continuous operation to a Mach number as high as 1.4 and provide choke-free flow in the test section throughout the transonic Mach number range. Constant Reynolds number can be maintained throughout the operational range of Mach numbers by controlling the stagnation pressure within the tunnel.

The models were mounted on a sting-supported flexure-type balance which was enclosed within the model bodies. The balance employed electrical-resistance strain gages to measure the forces and moments on the models.

Tests

Lift, pitching-moment, and drag data were obtained for both models at 20 Mach numbers ranging from 0.60 to 1.40 and for angles of attack ranging from -2° to approximately 15°. The Reynolds number of these data was held constant at a value of 1.5 million, based on the wing mean aerodynamic chord, except for some of the test points at the higher Mach numbers. For these points either the loads on the balance or the power supplied to the wind-tunnel drive motors reached limiting values, and the Reynolds number was reduced to 1.0 million. Further tests were made in which the minimum drag of each model was measured for Mach numbers varying from 0.60 to 1.40 at a constant Reynolds number of 1.5 million, and for Reynolds numbers varying from 1.0 million to about 3.0 or 4.0 million at a constant Mach number of 0.60.

The measurements were made with the models in the free- and fixed-transition conditions. The visualization technique described in reference 2 was used in brief tests to determine the locations of natural transition on the models for representative Mach numbers and incidences, and to determine the effectiveness of the wires in producing transition.

CORRECTIONS AND PRECISION

No wall-interference corrections have been applied to the data of this report. An evaluation of porous-wall interference in the Ames 2- by 2-Foot Transonic Wind Tunnel, reported in reference 1, has indicated that the interference is generally small for an unswept-wing model which was the same size as the models of the present investigation. Accordingly, the wall corrections to the present data are believed to be small also.

Several other factors which could have influenced the data have been considered and have been dealt with in various ways. Stream-angularity corrections were insignificant and are not included in the data. The axial forces measured by the internal balance have been adjusted to correspond to a condition of free-stream static pressure at the base of the body.

The drag coefficients measured with transition fixed have not been corrected for the pressure drag due to the wires. This pressure drag could not be determined from tests of the model with and without the wires. It was approximated, however, by the procedure described in reference 1, which consists essentially of estimating the pressures on both the upstream and downstream sides of the wires from measurements of pressures on forward and rearward facing steps. For a wire on the body nose and on both surfaces of the wing the estimated pressure-drag coefficients varied over the test range of Mach numbers from 0.0004 to 0.0006 for the swept-wing model and from 0.0004 to 0.0005 for the triangular-wing model.

In addition to any systematic errors which may be introduced by the corrections that have been neglected, the test data are subject to random errors of measurement (or deviations from the most probable values) which influence the reliability of the data. The mean square errors or standard deviations in the Mach numbers, angles of attack, Reynolds numbers, and in the lift, pitching-moment, and drag coefficients reported herein have been evaluated by the methods of reference 3. Representative values are given in the following table:

Item	M = 0.60		M = 1.00		M = 1.40	
	$\alpha = 0.25^\circ$	$\alpha = 6^\circ$	$\alpha = 0.25^\circ$	$\alpha = 6^\circ$	$\alpha = 0.25^\circ$	$\alpha = 6^\circ$
M	±0.002	±0.002	±0.002	±0.002	±0.002	±0.002
α	$\pm.02^\circ$	$\pm.02^\circ$	$\pm.02^\circ$	$\pm.04^\circ$	$\pm.02^\circ$	$\pm.03^\circ$
R	$\pm.02\times10^6$	$\pm.02\times10^6$	$\pm.01\times10^6$	$\pm.01\times10^6$	$\pm.02\times10^6$	$\pm.02\times10^6$
C_L	±.002	±.004	±.001	±.007	±.001	±.005
C_m	±.002	±.004	±.001	±.007	±.001	±.006
C_D	±.0002	±.0004	±.0002	±.0011	±.0002	±.0010

RESULTS AND DISCUSSION

Basic Data

The basic lift, pitching-moment, and drag data for 10 of the 20 Mach numbers of the investigation are presented for the swept- and triangular-wing models in figures 2 and 3, respectively. The remainder of the basic data is on file at the Ames Research Center of the NASA and can be obtained upon request. No pronounced effects of fixing transition are indicated by the data of figures 2 and 3 except for the expected increases in drag coefficient. In general, the data appear to be typical for the particular configurations, except for the abrupt jogs for the triangular-wing model evident in figure 3 for subsonic Mach numbers, and especially for Mach numbers from 0.90 to 0.98.

In the course of checking the validity of the jogs, the present data were compared with transition-free data reported in reference 4, which includes data for two models identical in every respect to the models of this report except that NACA 0003 wing sections were employed instead of biconvex sections. No abrupt jogs were evident in the lift, pitching-moment, and drag data for the triangular-wing model of reference 4, although in other respects the data were nearly the same as those for the triangular-wing model of this report. A search, however, of other published data (refs. 5 to 12) disclosed jogs in the aerodynamic characteristics of other triangular-wing configurations having either sharp or rounded leading edges and, furthermore, indicated that the occurrence of the jogs is influenced by the wing leading-edge contour (radius, thickness ratio of the wing, and camber) and by the amount of leading-edge sweep. In addition a check of the reduction of the present data from the balance readings showed that the jogs are not due to computational errors but stem directly from the balance readings. Accordingly, the jogs are considered to be valid aerodynamic characteristics of the present triangular wing, and the discrepancies between the data of reference 4 and the present investigation are attributed to the difference in the section profile of the two wings (NACA 0003 airfoil section vs. biconvex).

As a matter of interest, a comparison of the transition-free data for the 45° swept wing of reference 4 with the corresponding data of the present report showed that the lift characteristics were essentially the same for the two models, but the pitching-moment coefficients for a constant lift were somewhat more negative for the present model with biconvex sections. No drag data were presented in reference 4 for the swept-wing configuration.

Lift and Pitching-Moment Curve Slopes

Variations of the lift and pitching-moment curve slopes with Mach number as affected by fixing transition are shown in figures 4 and 5 for the swept- and triangular-wing models, respectively. (All the basic data have been used in the preparation of these figures.) The only significant effect of fixing transition for both models is the slight reduction in the magnitude of the variations of pitching-moment curve slope with Mach number at zero lift for subsonic Mach numbers greater than about 0.7 or 0.8. This result is in contrast with those found for the unswept-wing model in reference 1. For this model large effects of fixing transition were generally observed for both the lift and pitching-moment curve slopes at subsonic and transonic Mach numbers, and abrupt changes in the lift and pitching-moment curve slopes were smoothed out considerably for the fixed-transition condition. It appears, then, that significant effects of fixing transition with regard to the lift and pitching-moment curve slopes would be confined to wing plan forms with little or no sweep.

Minimum Drag Characteristics

The variations of minimum drag coefficient with Mach number and Reynolds number are presented in figure 6 for the swept- and triangular-wing models in both the fixed- and free-transition conditions. Also shown in this figure are calculated curves of minimum drag coefficient as a function of Reynolds number for each model with completely turbulent and completely laminar boundary layers. These calculated drag coefficients were determined from flat-plate incompressible-flow skin-friction coefficients which were considered to act over the wetted areas of the models. For the turbulent boundary layer, skin-friction coefficients from reference 13 were employed, which were corrected to a Mach number of 0.60 by the data of reference 14. For the laminar boundary layer the skin-friction coefficients were obtained from the expression $1.328R^{-1/2}$, and no Mach number correction was made.

It is evident in figures 6(a) and (b) that fixing the transition produced a nearly uniform increment in minimum drag coefficient over the range of Mach numbers from 0.60 to 1.40 for each model. Also, the magnitudes of the increments for the two models are essentially the same.

These magnitudes, however, are not to be expected at full-scale Reynolds numbers, since in figures 6(c) and (d) it is noted that the magnitude of the increments decreases substantially for each model as Reynolds number is increased to the highest values shown. This decrease is due largely to the apparent forward movement of the location of natural transition on the models as Reynolds number is increased from 1.0 million to about 3.0 or 4.0 million. Such a forward movement is indicated by the trend of the transition-free data relative to the calculated data for turbulent and laminar boundary layers. Only for the fixed-transition case are the effects of Reynolds number on the measured drag coefficients for each model closely approximated by the appropriate calculated values. This indicates, as a result, that the present minimum drag data could be extrapolated to full-scale values much more reliably when the transition is fixed rather than left free. These results for the minimum drag coefficient are identical with those noted in reference 1 for the unswept-wing model and, therefore, are apparently unaffected by changes in wing plan form.

A
3
3
3

Transition Characteristics of the Wings

The brief tests conducted throughout the Mach number range from 0.60 to 1.40 to examine visually the boundary-layer characteristics on the wings indicated that natural boundary-layer transition did not occur on either wing at zero incidence. As little as about 1° incidence, however, was generally sufficient to produce transition essentially at the leading edge on the upper surface of either wing. For further increases in incidence, transition remained at the leading edge of either wing, with the following exceptions: for the swept wing, at incidences from 4° to 10° for a Mach number of 1.20 and at about 2° to 14° for a Mach number of 1.40; and for the triangular wing, from 4° to 10° for a Mach number of 1.40. At the excepted incidences and Mach numbers for both wings, the flow expanded over the leading edge and transition on the upper surface was then delayed until the flow reached the oblique waves from the wing-body juncture.

On the lower surface of either wing, at 1° incidence, transition occurred at about the 90- to 100-percent chord position. As the incidence was increased to about 5°, transition moved upstream on each wing along a line roughly parallel to the leading edge, to a location approximately 25 or 30 percent of the root chord downstream of the leading edge. No further change in the location of transition was apparent as the angle of attack was increased from about 5° to 14°. These results for the lower surface were generally unaffected by Mach number between the limits of 0.60 and 1.40.

For the fixed-transition condition, tests throughout the Mach number range indicated that the wires were effective in causing transition on

both upper and lower surfaces of the wings at low angles of attack. Except where natural transition had already occurred upstream of the wires, transition was induced some 10 wire diameters downstream of the wire location.

The foregoing results provide an explanation for the generally small effects of fixing transition for the swept- and triangular-wing models. Except for incidences less than about 1°, natural transition on the upper surfaces of the wings was located so near the leading edge that all or essentially all of the flow was turbulent before reaching the transition wires. Accordingly, the wires served very little purpose on the upper surfaces of the wings. Since the effects of fixing transition arise primarily from corresponding changes in the characteristics of the flow over the upper surfaces, it is apparent that for the present swept and triangular wings such effects would necessarily be small.

CONCLUDING REMARKS

The results of the present investigation at transonic Mach numbers have indicated that the aerodynamic effects of fixing boundary-layer transition for the small-scale swept- and triangular-wing models, unlike the effects for the unswept-wing model of NACA TN 4228, were generally insignificant. Small reductions in the variations of the pitching-moment curve slopes with Mach number, however, were observed for the swept- and triangular-wing models at zero lift for subsonic Mach numbers greater than about 0.7 or 0.8. The insignificant effects due to fixing transition apparently result from the fact that the location of natural transition on the upper surface of the wings, except for very small incidences, was already either close to or upstream of the transition wire. Significant effects of fixing transition at transonic Mach numbers are apparently associated only with wings having little or no sweep.

The relatively large increments of minimum drag coefficient resulting from fixing transition on the swept- and triangular-wing configurations at Reynolds numbers of about 1.0 million were reduced considerably as the Reynolds number was increased to about 3.0 or 4.0 million. A comparable reduction in the increments of minimum drag coefficient with increase in Reynolds number was also observed for the unswept-wing configuration of NACA TN 4228. The agreement between the measured and calculated minimum drag coefficients as affected by Reynolds number has indicated that the measured values could be extrapolated to full-scale Reynolds numbers much more reliably when the transition was fixed.

Ames Research Center
National Aeronautics and Space Administration
Moffett Field, Calif., Dec. 31, 1959

REFERENCES

1. Stivers, Louis S., Jr., and Lippmann, Garth W.: Effects of Fixing Boundary-Layer Transition for an Unswept-Wing Model and an Evaluation of Porous Tunnel-Wall Interference for Mach Numbers from 0.60 to 1.40. NACA TN 4228, 1958.

2. Main-Smith, J. D.: Chemical Solids as Diffusible Coating Films for Visual Indications of Boundary-Layer Transition in Air and Water. British R. & M. No. 2755, 1950.

3. Beers, Yardley: Introduction to the Theory of Error. Addison-Wesley Publishing Co., Cambridge, Mass., 1953.

4. Knechtel, Earl D., and Summers, James L.: Effects of Sweep and Taper Ratio on the Longitudinal Characteristics of an Aspect Ratio 3 Wing-Body Combination at Mach Numbers from 0.6 to 1.4. NACA RM A55A03, 1955.

5. Edwards, George G., and Stephenson, Jack D.: Tests of a Triangular Wing of Aspect Ratio 2 in the Ames 12-Foot Pressure Wind Tunnel. I - The Effect of Reynolds Number and Mach Number on the Aerodynamic Characteristics of the Wing with Flap Undeflected. NACA RM A7K05, 1948.

6. Heitmeyer, John C., and Stephenson, Jack D.: Lift, Drag, and Pitching Moment of Low-Aspect-Ratio Wings at Subsonic and Supersonic Speeds - Plane Triangular Wing of Aspect Ratio 4 with NACA 0005-63 Section. NACA RM A50K24, 1951.

7. Phelps, E. Ray, and Smith, Willard G.: Lift, Drag, and Pitching Moment of Low-Aspect-Ratio Wings at Subsonic and Supersonic Speeds - Triangular Wing of Aspect Ratio 4 with NACA 0005-63 Thickness Distribution, Cambered and Twisted for Trapezoidal Span Load Distribution. NACA RM A50K24b, 1951.

8. Heitmeyer, John C.: Lift, Drag, and Pitching Moment of Low-Aspect-Ratio Wings at Subsonic and Supersonic Speeds - Plane Triangular Wing of Aspect Ratio 4 with 3-Percent-Thick Biconvex Section. NACA RM A51D30, 1951.

9. Burrows, Dale L., and Palmer, William E.: A Transonic Wind-Tunnel Investigation of the Longitudinal Force and Moment Characteristics of a Plane and a Cambered 3-Percent-Thick Delta Wing of Aspect Ratio 3 on a Slender Body. NACA RM L54H25, 1954.

10. Burrows, Dale L., and Tucker, Warren A.: A Transonic Wind-Tunnel Investigation of the Static Longitudinal Characteristics of a 3-Percent-Thick, Aspect-Ratio-3, Delta Wing Cambered and Twisted for High Lift-Drag Ratios. NACA RM L55F02a, 1955.

11. Mugler, John P.: Transonic Wind-Tunnel Investigation of the Aerodynamic Loading Characteristics of a 60° Delta Wing in the Presence of a Body With and Without Indentation. NACA RM L55G11, 1955.

12. Sutton, E. P.: Some Observations of the Flow over a Delta Winged Model With 55° Leading-Edge Sweep at Mach Numbers Between 0.4 and 1.8. British RAE TN Aero. 2430, 1955.

13. Locke, F. W. S., Jr.: Recommended Definition of Turbulent Friction in Incompressible Fluids. Bur. Aer., Navy Dept., (Design) Res. Div., DR Rep. 1415, 1952.

14. Chapman, Dean R., and Kester, Robert H.: Turbulent Boundary-Layer and Skin-Friction Measurements in Axial Flow Along Cylinders at Mach Numbers Between 0.5 and 3.6. NACA TN 3097, 1954.

A
3
3
3

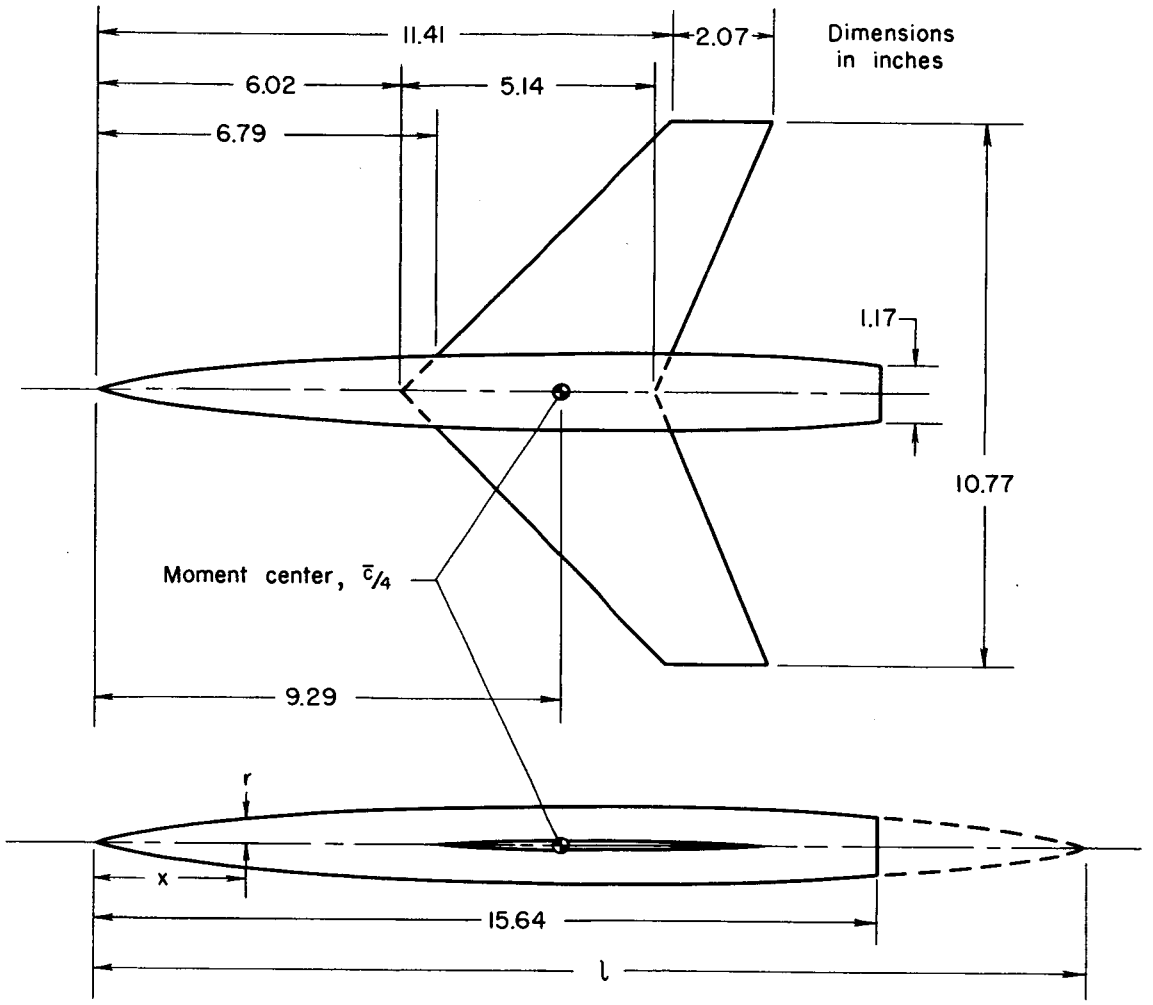

Wing	
Aspect ratio	2.99
Taper ratio	.40
Thickness-chord ratio	.03
Airfoil section	Biconvex
Area	38.83 sq. in.
Mean aerodynamic chord	3.82 in.
Leading-edge sweepback	45°

Body

Ordinates given by:

$$\frac{r}{r_o} = \left[1 - \left(1 - \frac{2x}{l}\right)^2\right]^{\frac{3}{4}}$$

Where:

r = local radius

$r_o = r_{maximum} = 0.794$ in.

x = longitudinal distance from nose

$l = 2(x_{for\ r_o}) = 19.833$ in.

(a) Swept-wing model.

Figure 1.- Geometrical information for the models.

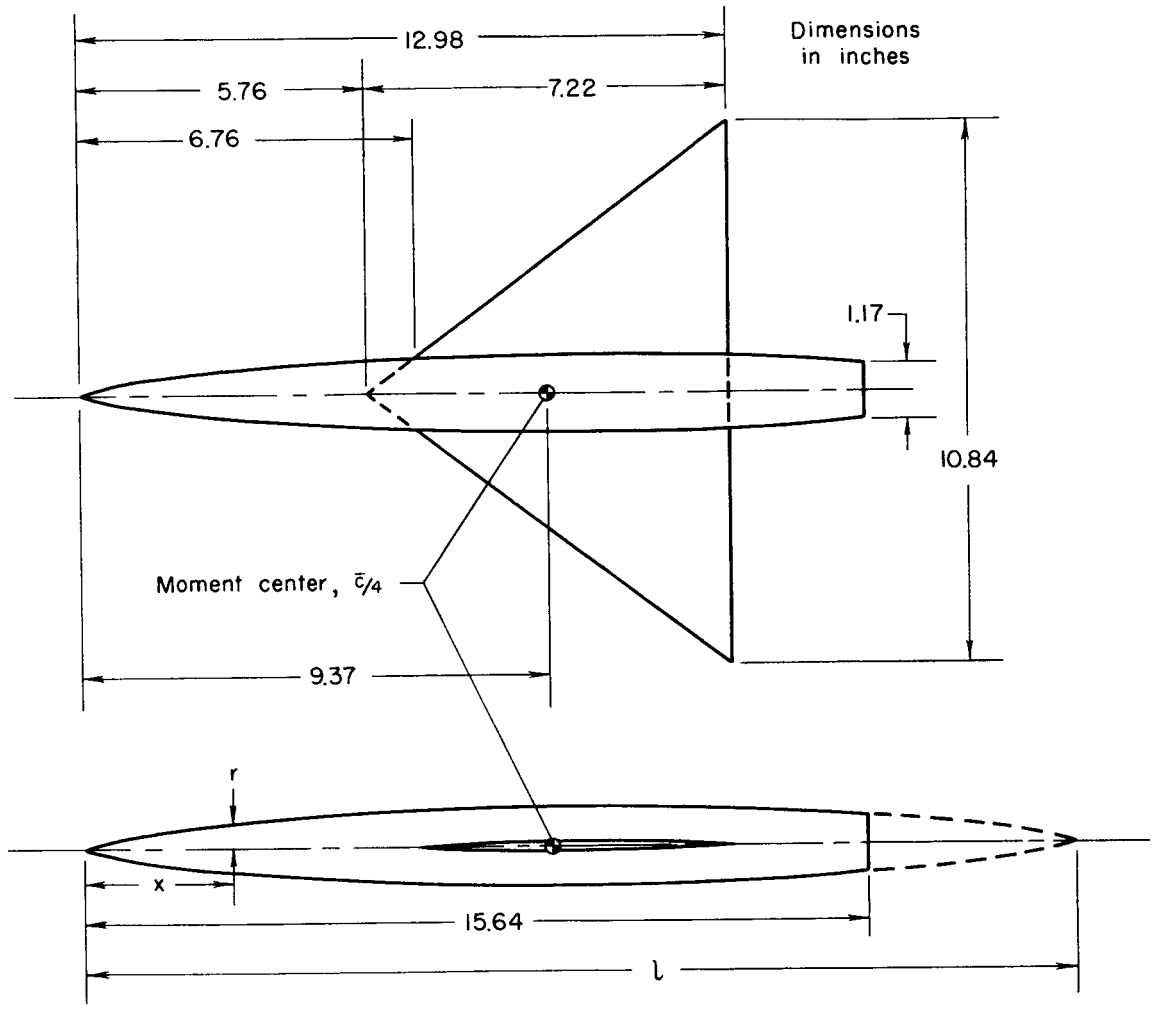

Wing	
Aspect ratio	2.99
Taper ratio	0
Thickness-chord ratio	.03
Airfoil section	Biconvex
Area	39.23 sq in.
Mean aerodynamic chord	4.81 in.
Leading-edge sweepback	53.1°

Body

Ordinates given by:

$$\frac{r}{r_o} = \left[1 - \left(1 - \frac{2x}{l}\right)^2\right]^{\frac{3}{4}}$$

Where:

r = local radius

$r_o = r_{maximum} = 0.794$ in.

x = longitudinal distance from nose

$l = 2(x_{for\ r_o}) = 19.833$ in.

(b) Triangular-wing model.

Figure 1.- Concluded.

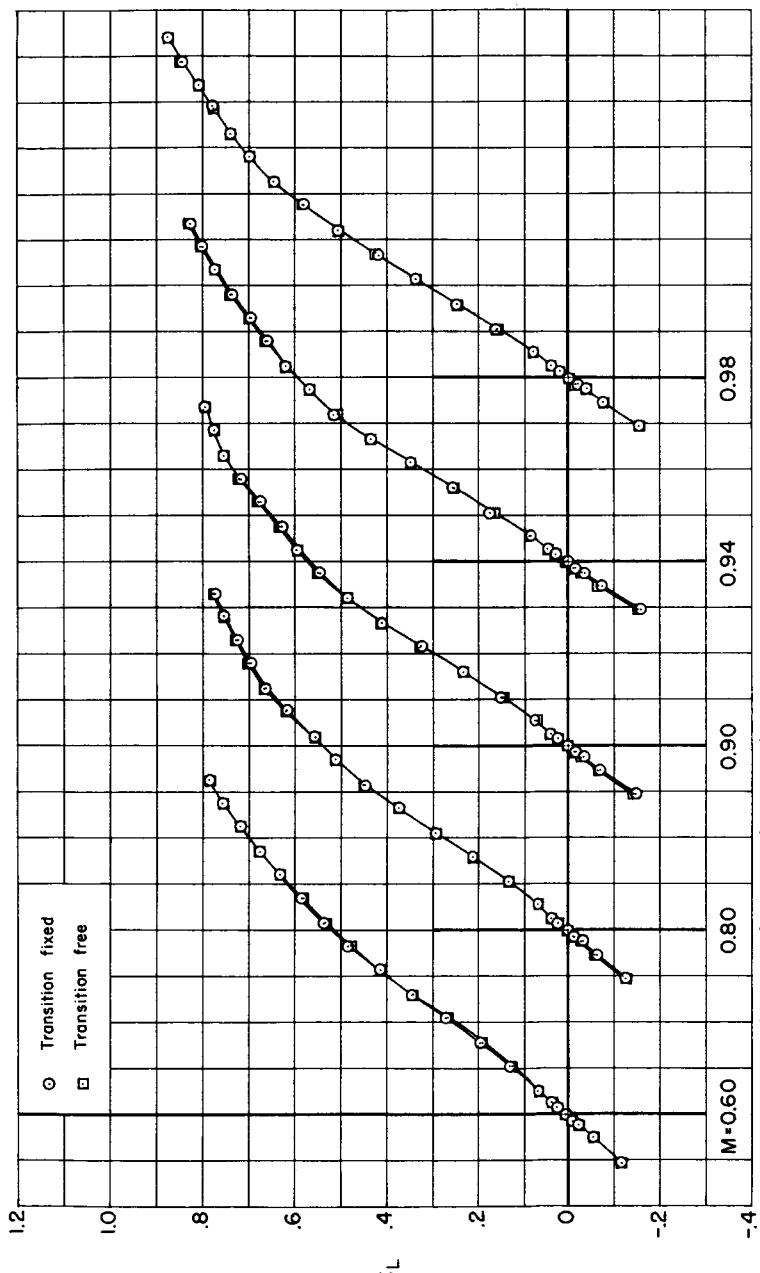

(a) C_L vs. α; subsonic Mach numbers.

Figure 2.- Basic aerodynamic characteristics for the swept-wing model; R = 1.5×10^6 (flags indicate R = 1.0×10^6).

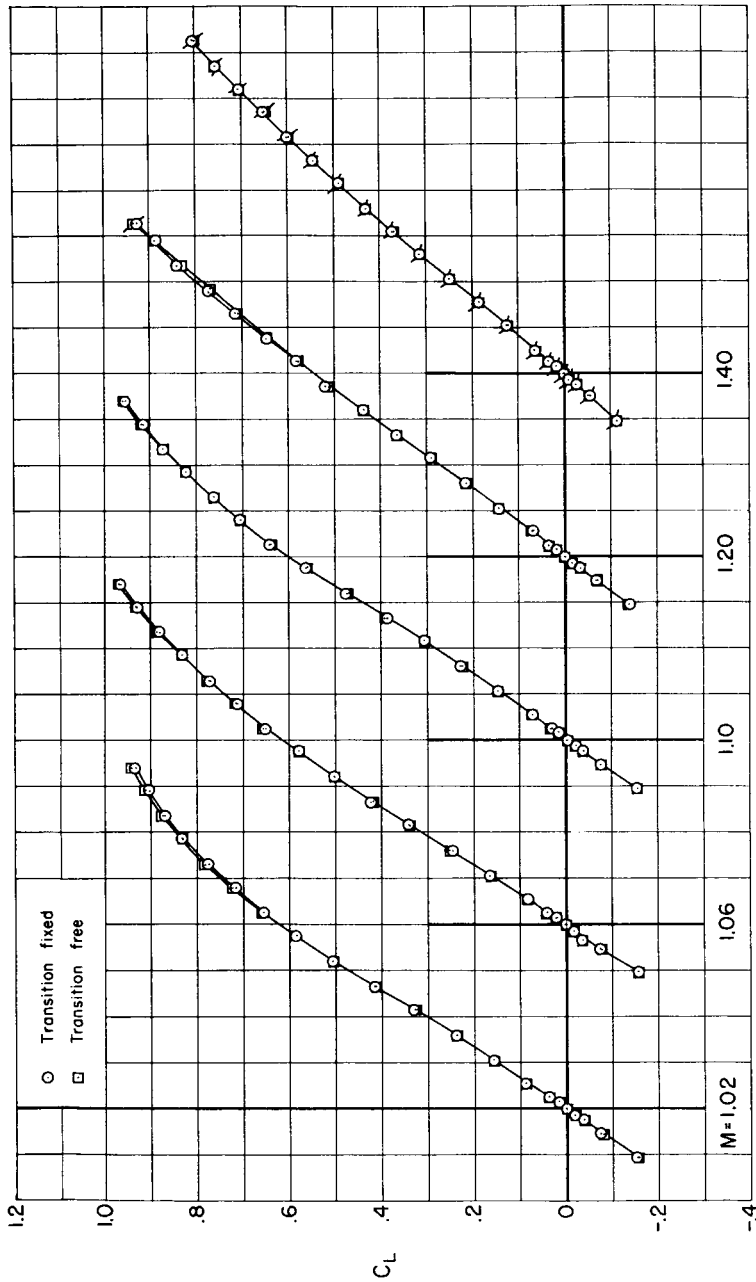

(b) C_L vs. α; supersonic Mach numbers.

Figure 2.- Continued.

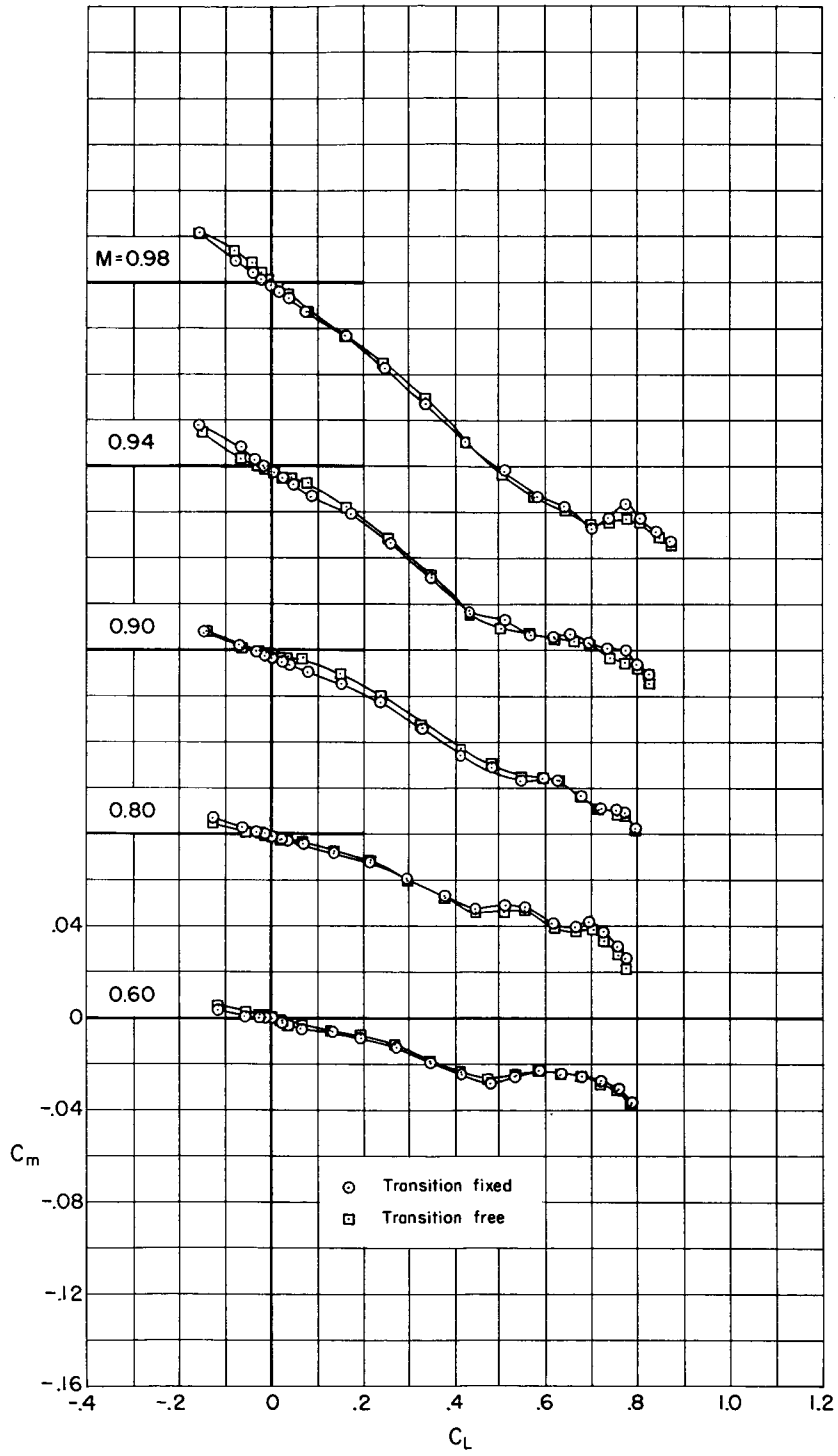

(c) C_m vs. C_L; subsonic Mach numbers.

Figure 2.- Continued.

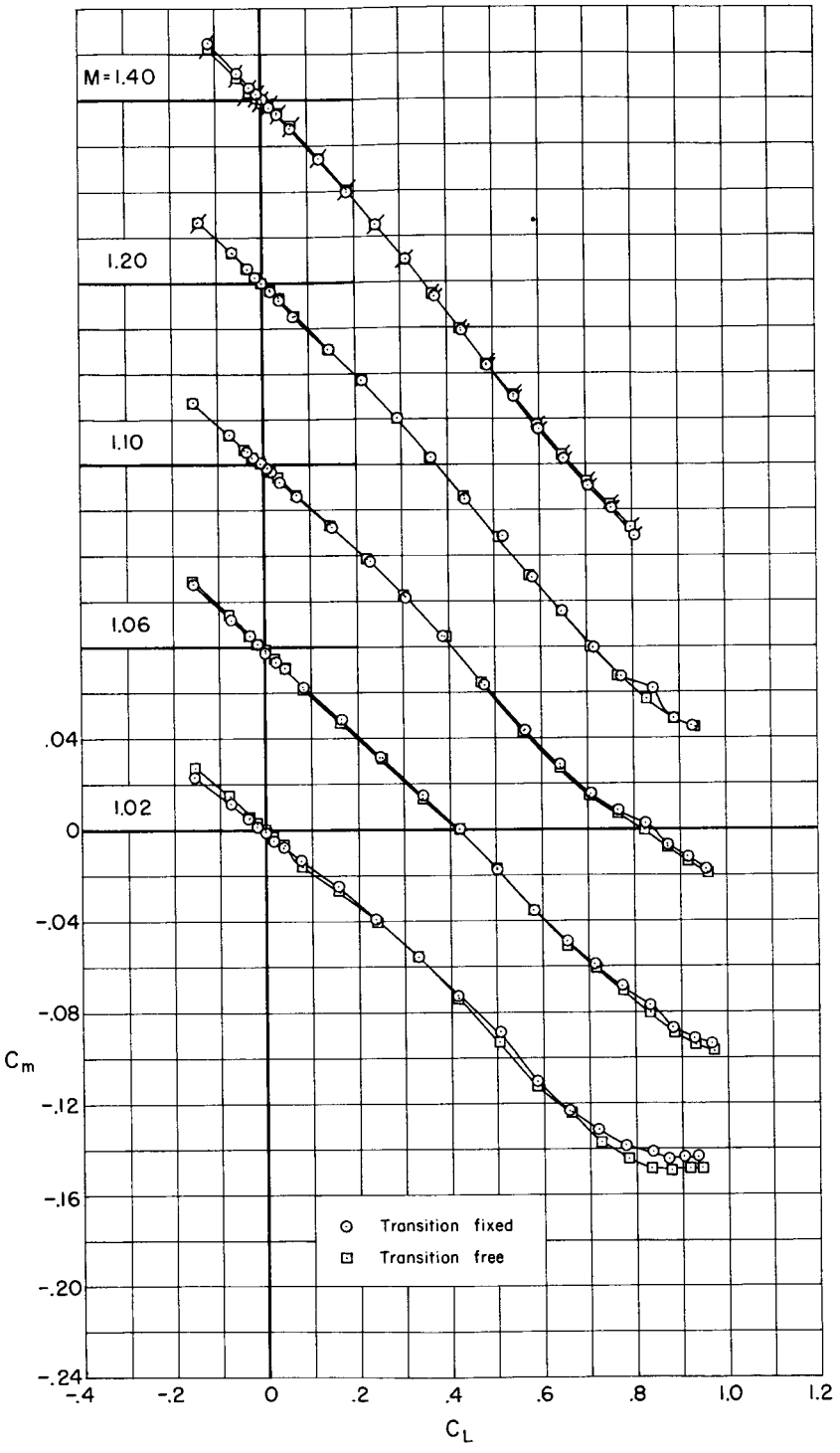

(d) C_m vs. C_L; supersonic Mach numbers.

Figure 2.- Continued.

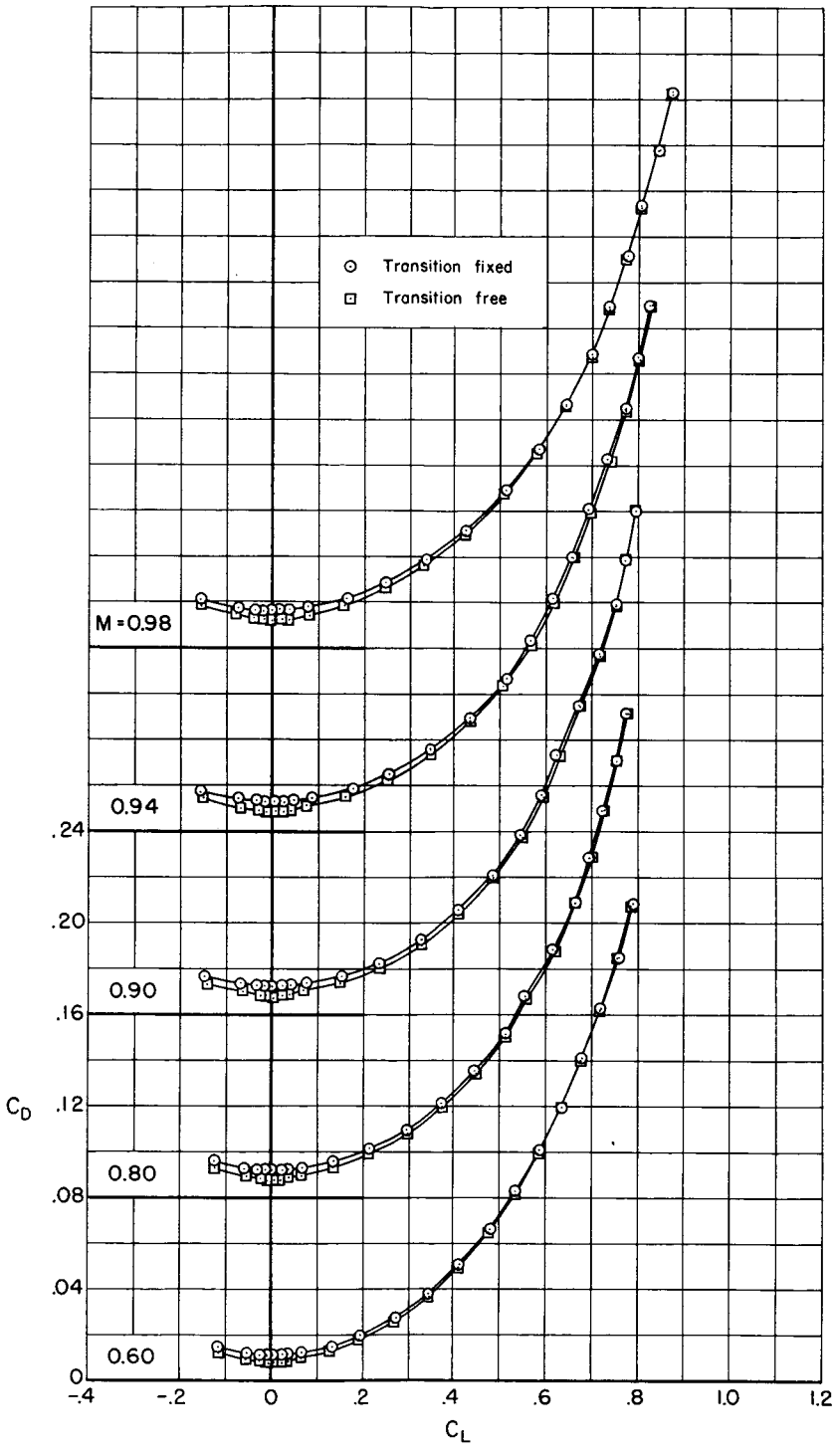

(e) C_D vs. C_L; subsonic Mach numbers.

Figure 2.- Continued.

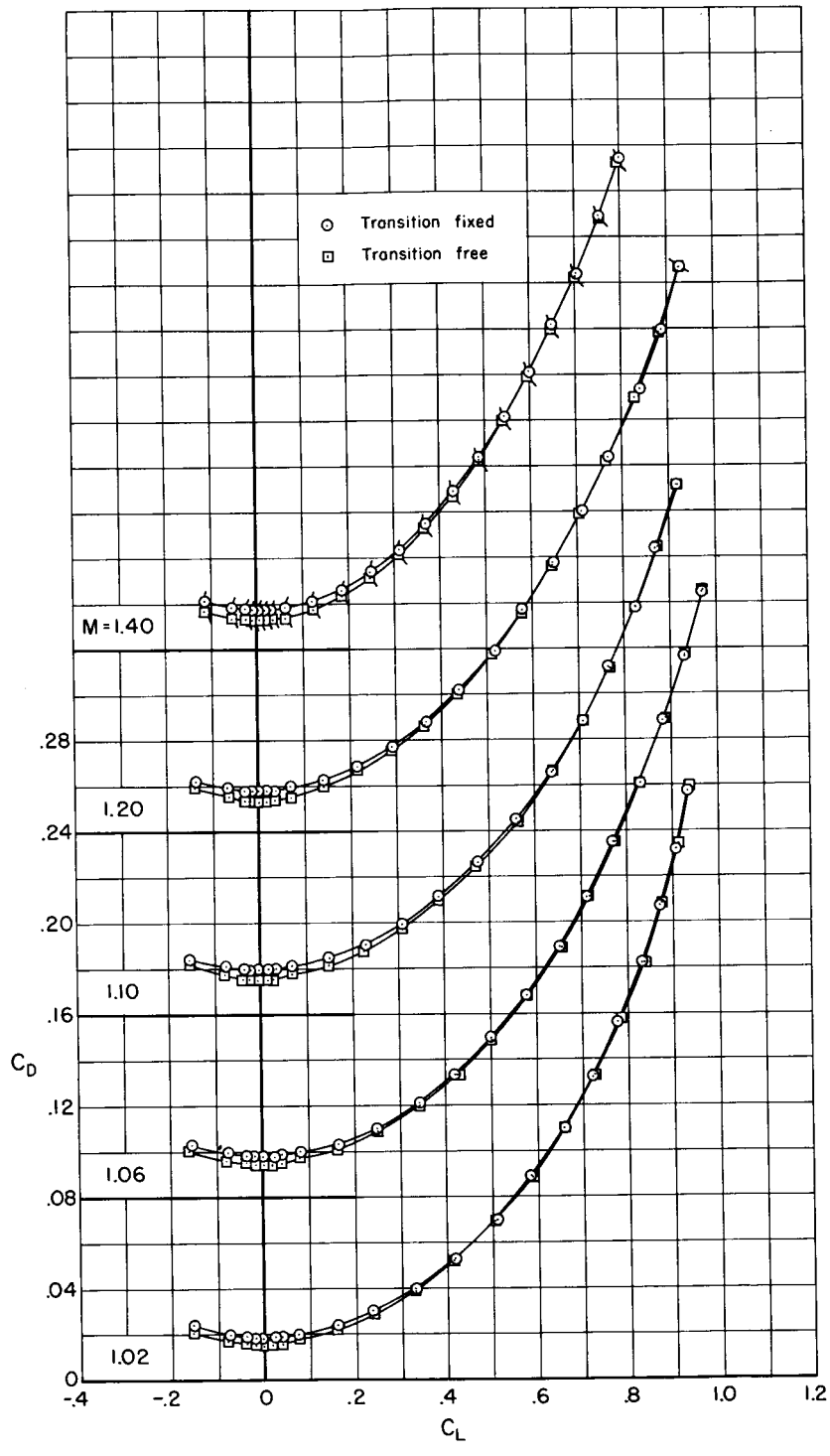

(f) C_D vs. C_L; supersonic Mach numbers.

Figure 2.- Concluded.

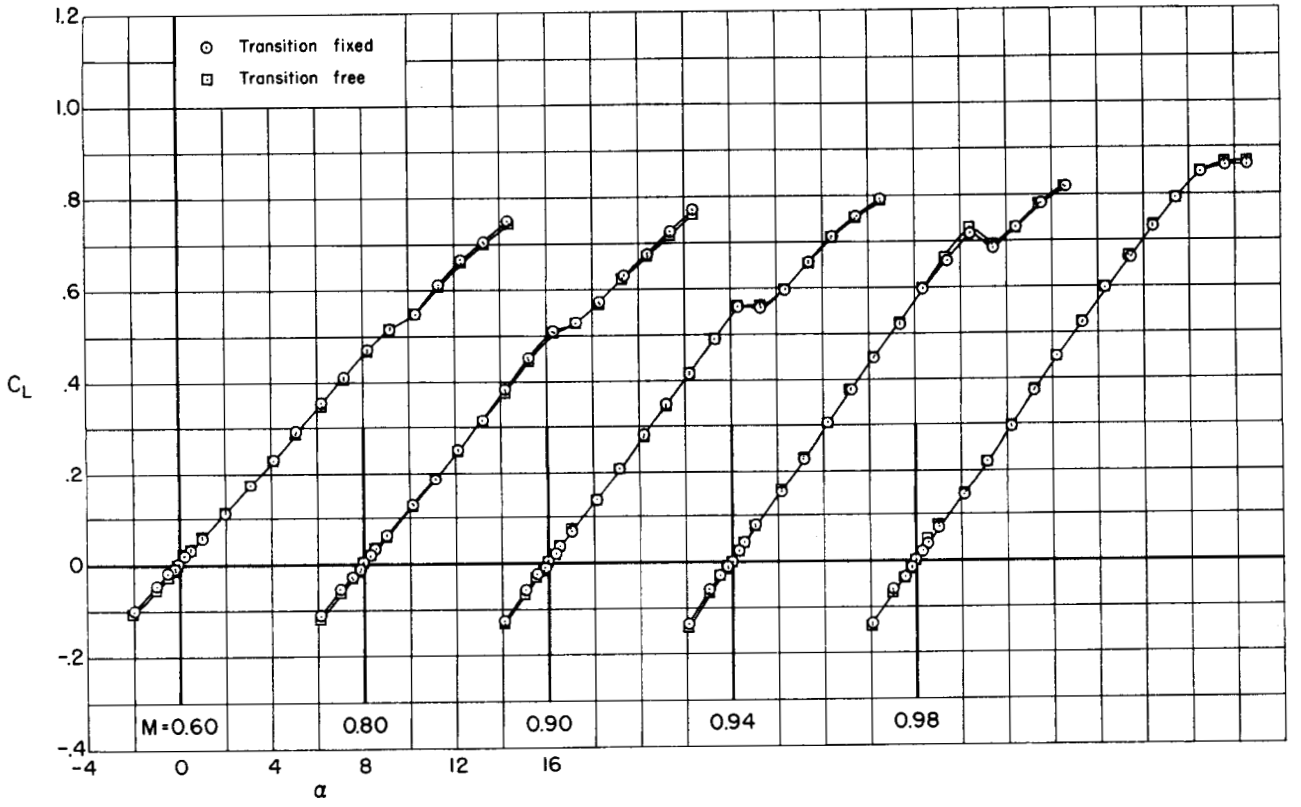

(a) C_L vs. α; subsonic Mach numbers.

Figure 3.- Basic aerodynamic characteristics for the triangular-wing model; R = 1.5×10^6.

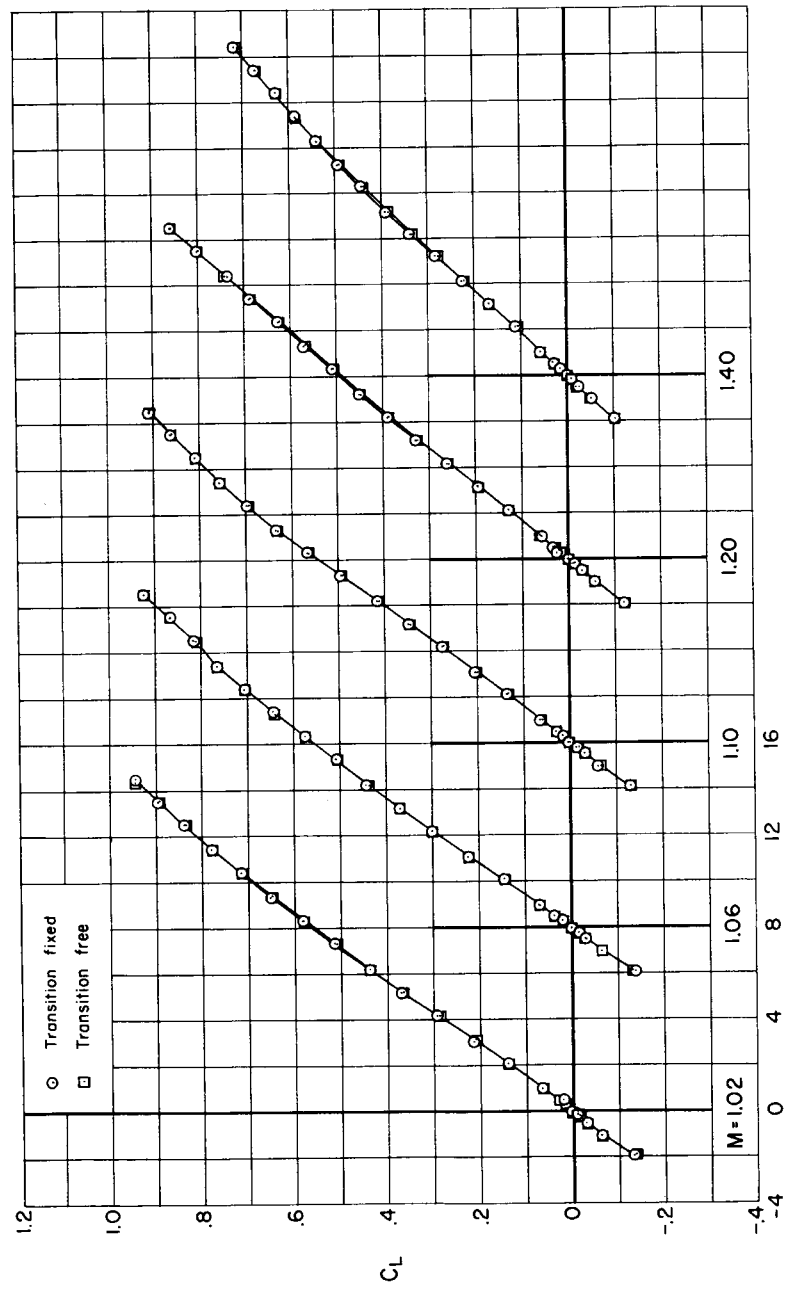

(b) C_L vs. α; supersonic Mach numbers.

Figure 3.- Continued.

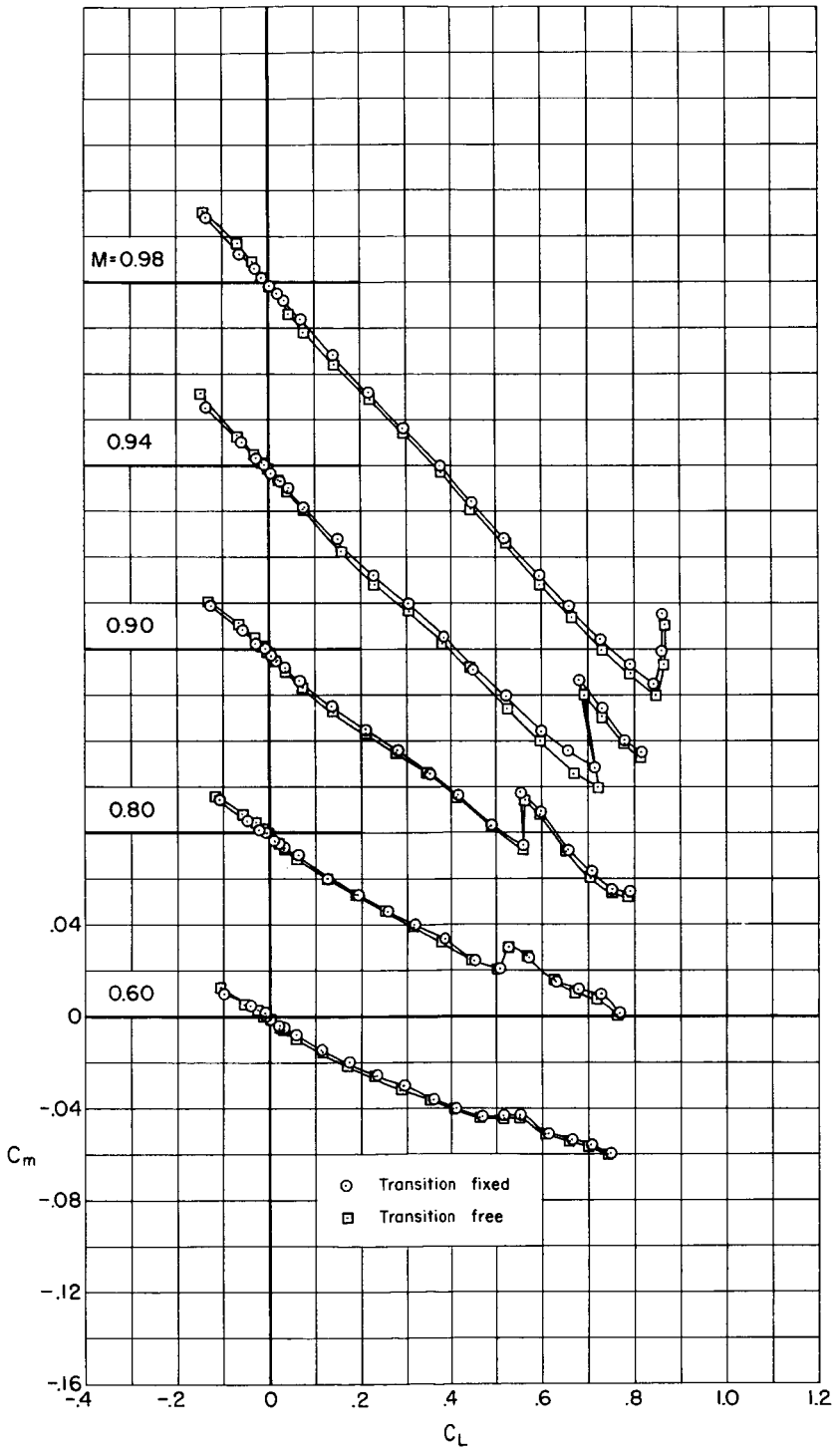

(c) C_m vs. C_L; subsonic Mach numbers.

Figure 3.- Continued.

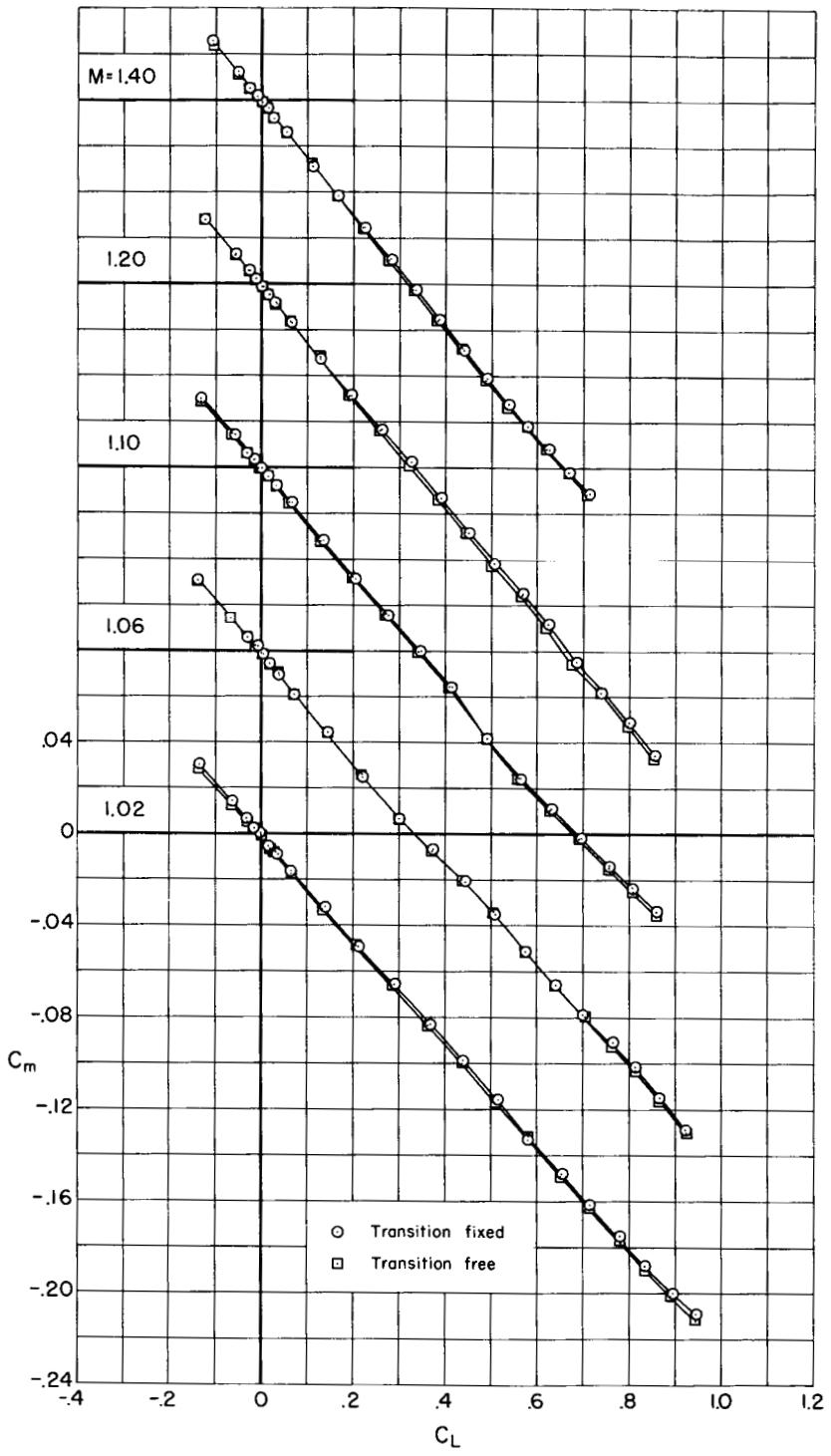

(d) C_m vs. C_L; supersonic Mach numbers.

Figure 3.- Continued.

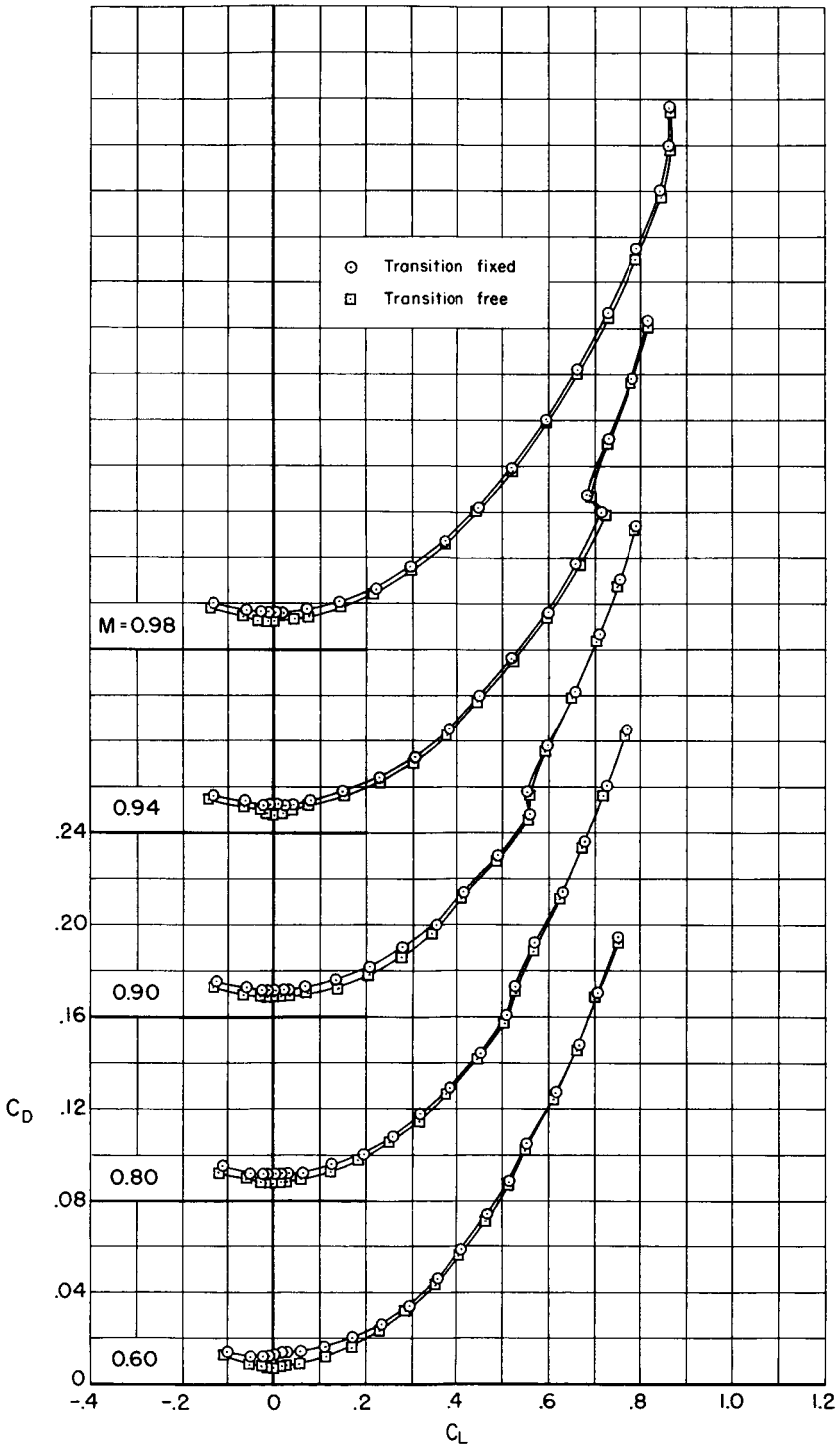

(e) C_D vs. C_L; subsonic Mach numbers.

Figure 3.- Continued.

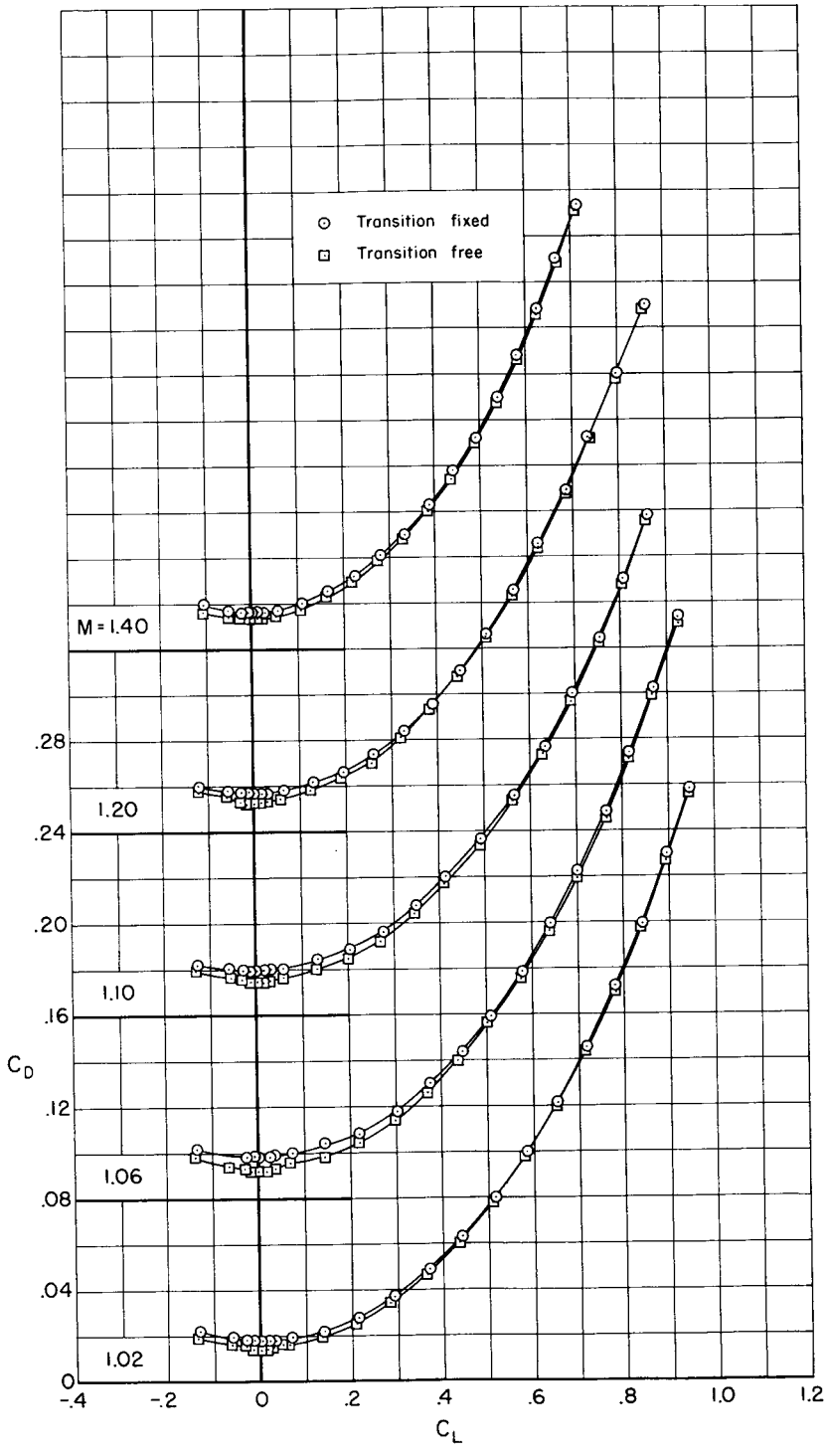

(f) C_D vs. C_L; supersonic Mach numbers.

Figure 3.- Concluded.

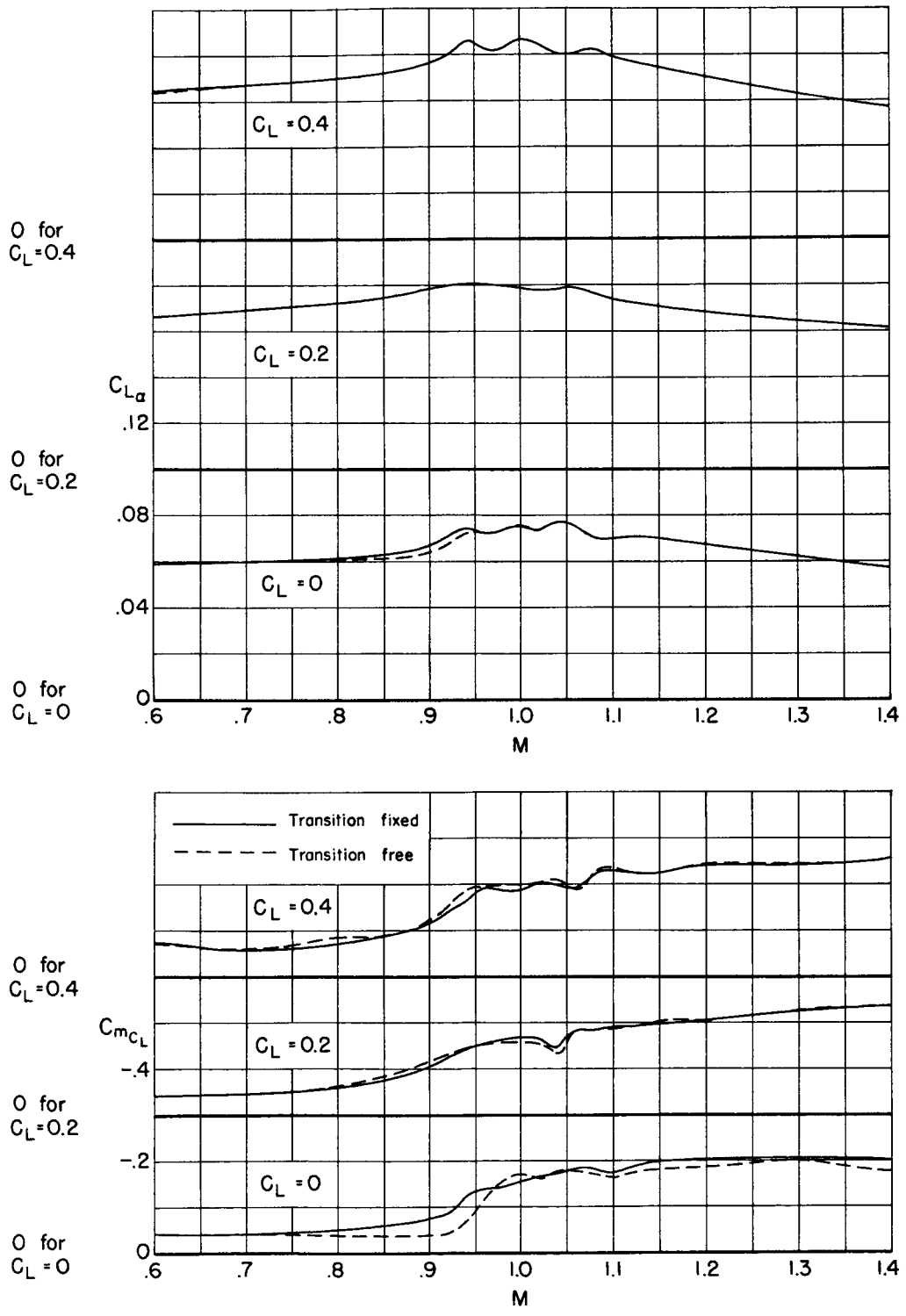

Figure 4.- Lift and pitching-moment curve slopes for the swept-wing model.

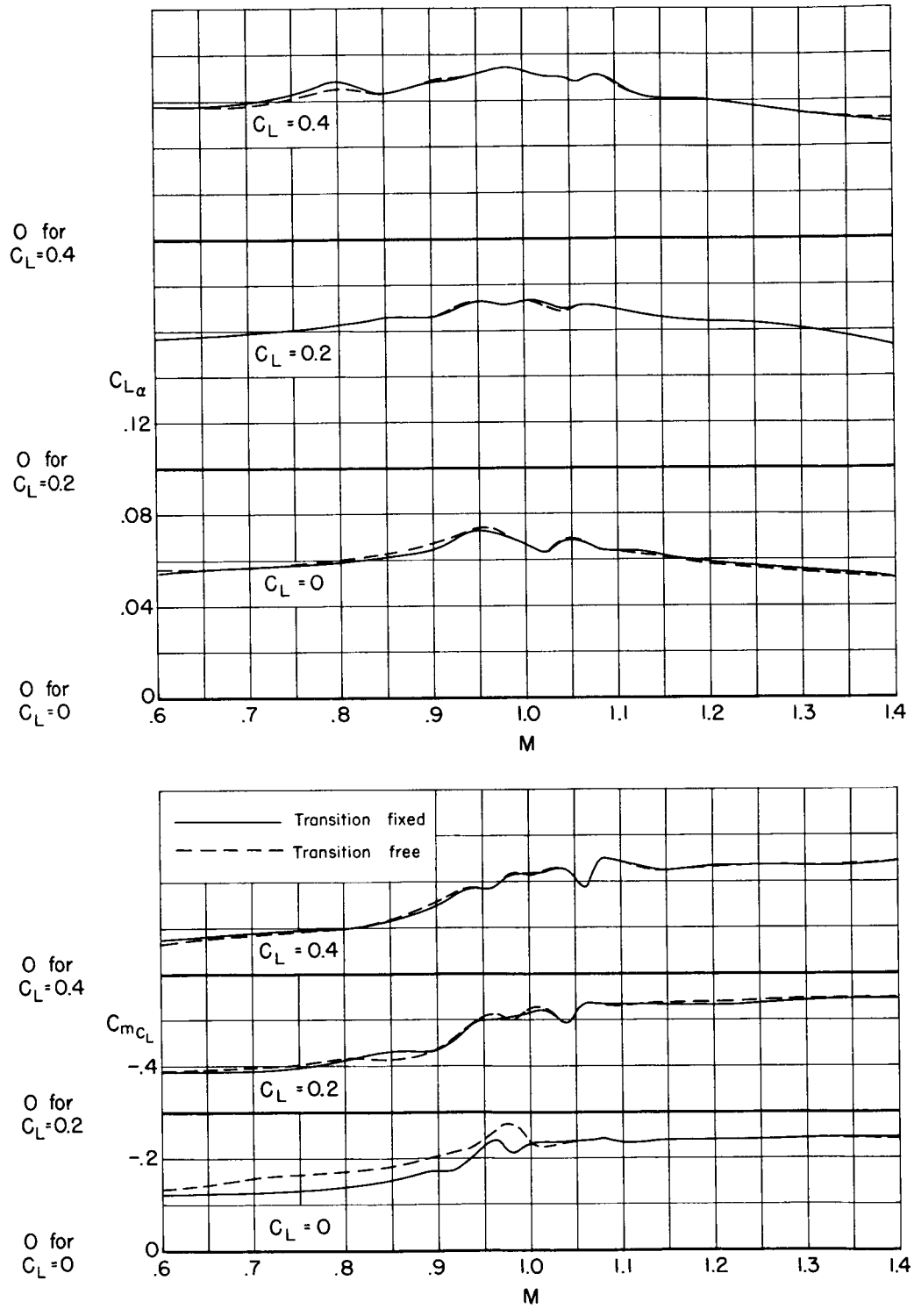

Figure 5.- Lift and pitching-moment curve slopes for the triangular-wing model.

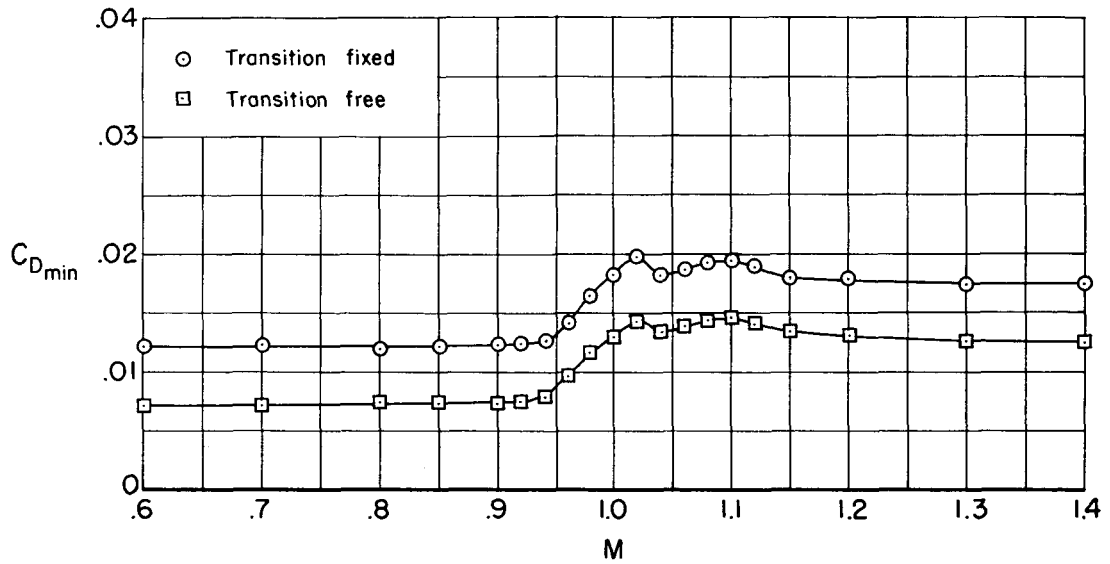

(a) $C_{D_{min}}$ vs. M; swept wing; R = 1.5×10^6.

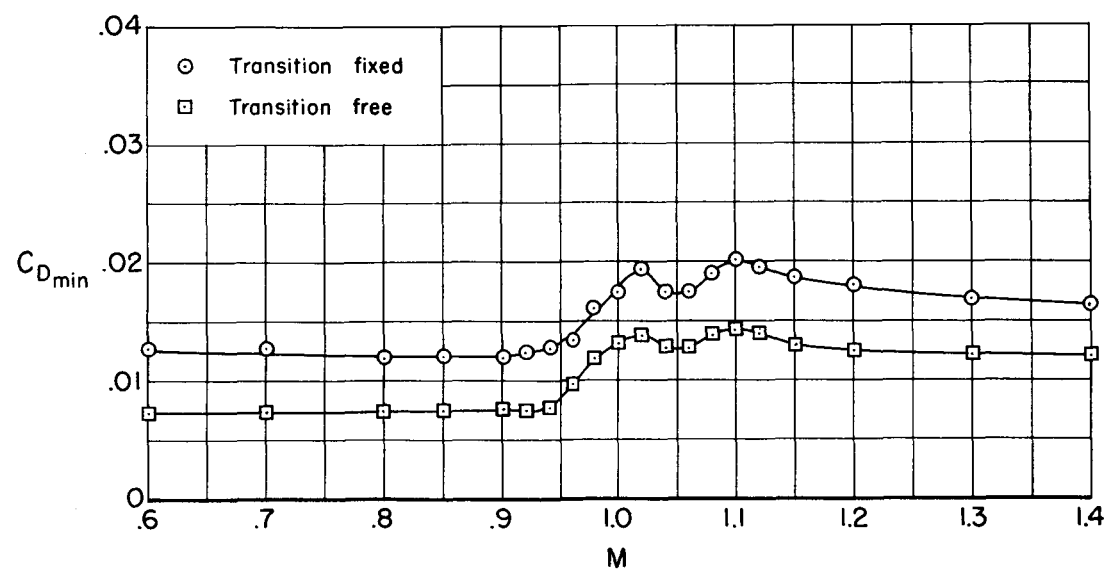

(b) $C_{D_{min}}$ vs. M; triangular wing; R = 1.5×10^6.

Figure 6.- Minimum drag characteristics for the swept- and triangular-wing models.

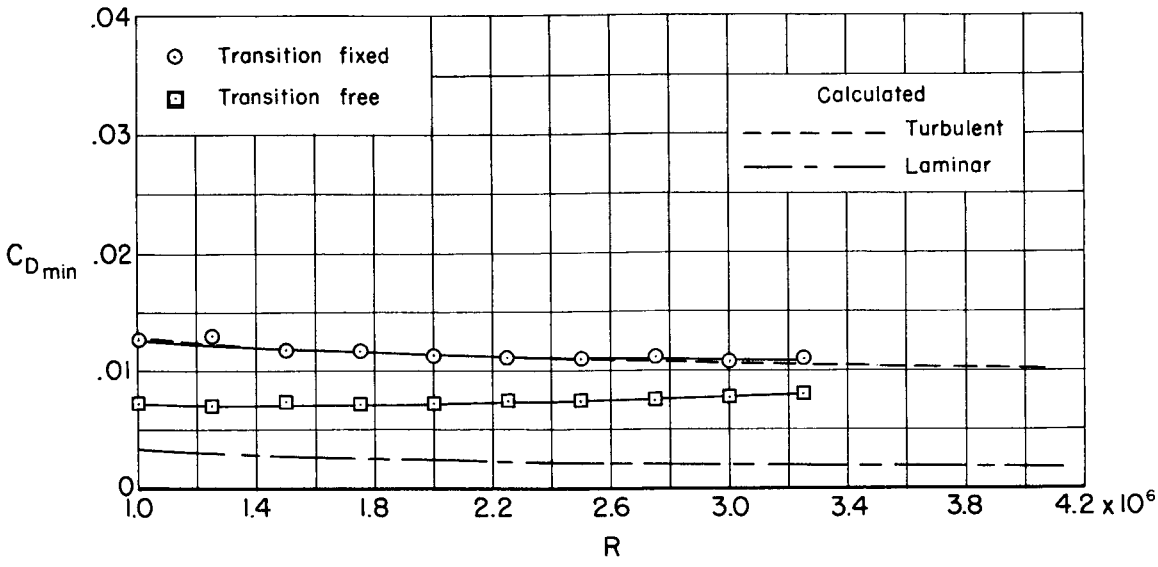

(c) $C_{D_{min}}$ vs. R; swept wing; M = 0.60.

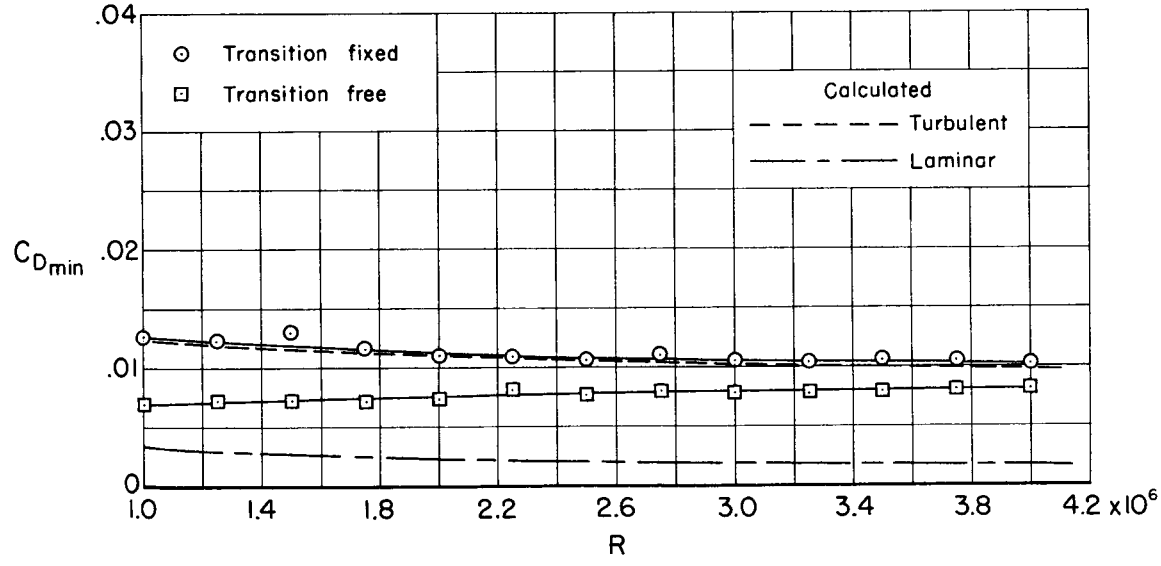

(d) $C_{D_{min}}$ vs. R; triangular wing; M = 0.60.

Figure 6.- Concluded.